

## Molecular Absorption Lines at High Redshift

Tommy Wiklind

*Onsala Space Observatory, S-43992 Onsala, Sweden*

Françoise Combes

*Observatoire de Paris, DEMIRM, 61 Av. de l'Observatoire  
F-75014 Paris, France*

**Abstract.** The four known molecular absorption line systems at redshifts  $z=0.25-0.89$  are discussed. Two of the systems originate in the galaxy hosting the ‘background’ AGN, while in two cases the absorption occurs in truly intervening galaxies. Indirect evidence for the existence of very small scale structure in the molecular ISM is presented. A new absorption line at  $z=0.89$  towards PKS1830-211 opens up interesting possibilities to accurately derive the mass of the lensing galaxy.

### 1. Introduction

Galaxy evolution in general and star formation in particular are directly associated with molecular gas. The study of this dense and cold component of the interstellar medium (ISM) in distant galaxies gives important information about the conditions for star formation at different epochs during the evolution of the universe. In this respect, molecular absorption and emission lines are complementary to each other. Whereas emission lines give information about global properties, such as the total gas content and rotational velocity, the absorption lines probe the molecular ISM in greater detail, with more sensitivity and on spatial scales limited only by the angular extent of the background source. In addition, emission and absorption lines probe different types of molecular gas.

**Emission.** The observed property for molecular *emission* is the velocity integrated line intensity, which for a galaxy at redshift  $z$  can be expressed as  $\int T_A^* dV \approx (\Omega_s/\Omega_b) T_b \Delta V (1+z)^{-1}$ . The ratio of the solid angle of the source,  $\Omega_s$ , and the telescope beam,  $\Omega_b$ , represents the beam filling factor (valid as long as  $\Omega_s \leq \Omega_b$ ).  $T_b$  is the intrinsic brightness temperature, where the observed intensity is diminished by  $(1+z)$  and  $\Delta V$  is the width of the profile. For optically thick emission, the brightness temperature is  $T_b = [J(T_x) - J(T_{bg})]$ , where  $J(T) = (h\nu/k) / \{\exp(h\nu/k) - 1\}^{-1}$ .  $T_x$  and  $T_{bg}$  are the excitation temperature and the temperature of the cosmic background radiation, respectively. For  $T_x$  somewhat higher than  $T_{bg}$ , the brightness temperature is approximately proportional to  $T_x$ , while it vanishes when  $T_x \rightarrow T_{bg}$ . For a fixed-size galaxy, the observed integrated line intensity  $\int T_A^* dV \propto \Omega_b^{-1} (1+z)^3 D_L^{-2} \Delta V T_x$ , where  $D_L$  is the luminosity distance.

**Absorption.** The observed property of a molecular *absorption* line is the velocity integrated opacity. Assuming that the population of rotational levels can be described by a single temperature  $T_{\text{rot}} = T_x$ , not necessarily equal to the kinetic temperature, the integrated opacity can be expressed as:

$$\int \tau_\nu dv \propto \frac{N_{\text{tot}}}{T_x} \mu_0^2 (1 - \exp(-h\nu/kT_x)) \approx \frac{N_{\text{tot}}}{T_x^2} \mu_0^2 ,$$

where  $N_{\text{tot}}$  is the total column density of the molecule in question and  $\mu_0$  the permanent dipole moment. This expression is strictly speaking true only for linear molecules and transitions from the ground state for which  $h\nu \ll kT_x$ , but is similar for more complex species and higher order transitions.

This different dependence on the excitation temperature for absorption and emission lines illustrates how absorption measurements are sensitive to excitationally cold gas, whereas emission lines probe the warm gas. Under normal circumstances the excitation of molecular rotational transitions is dominated by collisions. An excitationally cold gas therefore corresponds to a diffuse gas component and warm gas to dense gas. The inverse quadratic dependence on  $T_x$  for absorption line observations can have profound influences on the estimates of total column densities, which will be discussed below. Furthermore, the observed integrated opacity does not include a distance dependence for the absorption line measurements. Instead the sensitivity only depends on the strength of the background continuum source. This means that the same kind of data that can be obtained in the Milky Way (e.g. Lucas & Liszt 1994, 1996), in Cen A at a distance of  $\sim 4$  Mpc (e.g. Wiklind & Combes 1997a) can be obtained towards PKS1830–211 at a luminosity distance  $\sim 4$  Gpc (Wiklind & Combes 1996a, 1997c).

Table 1. Properties of molecular absorption line systems.

Source	$z_a^a$	$z_e^b$	$N_{\text{CO}}$ $\text{cm}^{-2}$	$N_{\text{H}_2}$ $\text{cm}^{-2}$	$N_{\text{HI}}$ $\text{cm}^{-2}$	$A'_V{}^c$	$N_{\text{HI}}/N_{\text{H}_2}$
Cen A	0.00184	0.0018	$1.0 \times 10^{16}$	$2.0 \times 10^{20}$	$1 \times 10^{20}$	50	0.5
PKS1413+357	0.24671	0.247	$2.3 \times 10^{16}$	$4.6 \times 10^{20}$	$1.3 \times 10^{21}$	2.0	2.8
B3 1504+377A	0.67335	0.673	$6.0 \times 10^{16}$	$1.2 \times 10^{21}$	$2.4 \times 10^{21}$	5.0	2.0
B3 1504+377B	0.67150	0.673	$2.6 \times 10^{16}$	$5.2 \times 10^{20}$	$< 7 \times 10^{20}$	$< 2$	$< 1.4$
B 0218+357	0.68466	0.94	$2.0 \times 10^{19}$	$4.0 \times 10^{23}$	$4.0 \times 10^{20}$	850	$1 \times 10^{-3}$
PKS1830–211A	0.88582	?	$2.0 \times 10^{18}$	$4.0 \times 10^{22}$	$5.0 \times 10^{20}$	100	$1 \times 10^{-2}$
PKS1830–211B	0.88489	?	$1.0 \times 10^{16d}$	$2.0 \times 10^{20}$	$1.0 \times 10^{21}$	1.8	5.0
PKS1830–211C	0.19267	?	$< 6 \times 10^{15}$	$< 1 \times 10^{20}$	$2.5 \times 10^{20}$	$< 0.2$	$> 2.5$

<sup>a</sup>Redshift of absorption line

<sup>b</sup>Redshift of background source

<sup>c</sup>Extinction corrected for redshift using a Galactic extinction law

<sup>d</sup>Estimated from the  $\text{HCO}^+$  column density of  $1.3 \times 10^{13} \text{ cm}^{-2}$

<sup>e</sup>21cm HI data taken from Carilli et al. 1992, 1993, 1997a,b. A spin-temperature of 100 K and a area covering factor of 1 was assumed

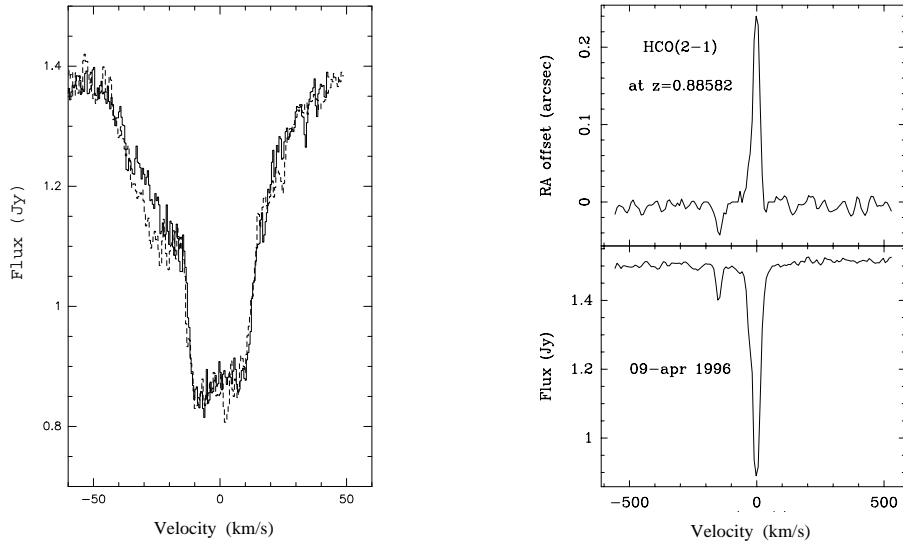


Figure 1.  $\text{HCO}^+(2-1)$  absorption at  $z=0.88582$  towards PKS1830–211 observed with the Plateau de Bure interferometer. **a)** High resolution spectrum at two different epochs (dashed/full drawn lines). **b)** Low resolution spectra (lower panel) showing two absorption line systems. The upper panel shows the shift in RA of the phase center relative to that of the unobscured continuum flux.

## 2. Known Molecular Absorption Line Systems

There are four known molecular absorption line systems at high redshift:  $z=0.25-0.89$ . These are listed in Table 1 together with data for the low redshift absorption system seen toward the radio core of Cen A. For the high redshift ones, a total of 15 different molecules have been detected, in a total of 29 different transitions. This includes several isotopic species:  $\text{C}^{13}\text{O}$ ,  $\text{C}^{18}\text{O}$ ,  $\text{H}^{13}\text{CO}$ ,  $\text{H}^{13}\text{CN}$ . As can be seen from Table 1, the inferred  $\text{H}_2$  column densities varies by  $\sim 10^3$ . The isotopic species are only detectable towards the systems with the highest column densities: B0218+357 and PKS1830–211. The large dispersion in column densities is reflected in the large spread in optical extinction  $A_V$  as well as the atomic to molecular ratio. Systems with high extinction have 10–100 times higher molecular gas fraction than those of low extinction. However, as discussed by Combes & Wiklind (these proceedings), the relation between HI and molecular gas along sightlines to background QSOs can be ambiguous.

*Absorption in the host galaxy.* Two of the four known molecular absorption line systems are situated within the host galaxy to the ‘background’ continuum source: PKS1413+135 and B3 1504+377. The latter exhibits two absorption line systems with similar redshifts,  $z=0.67150$  and  $0.67335$  (Wiklind & Combes 1996b). The separation in restframe velocity is  $330 \text{ km s}^{-1}$ . This is the type of signature one would expect from absorption occurring in a galaxy acting as a gravitational lens. However, in this case, as well as for PKS1413+135, high angular resolution VLBI images show no image multiplicity, despite impact pa-

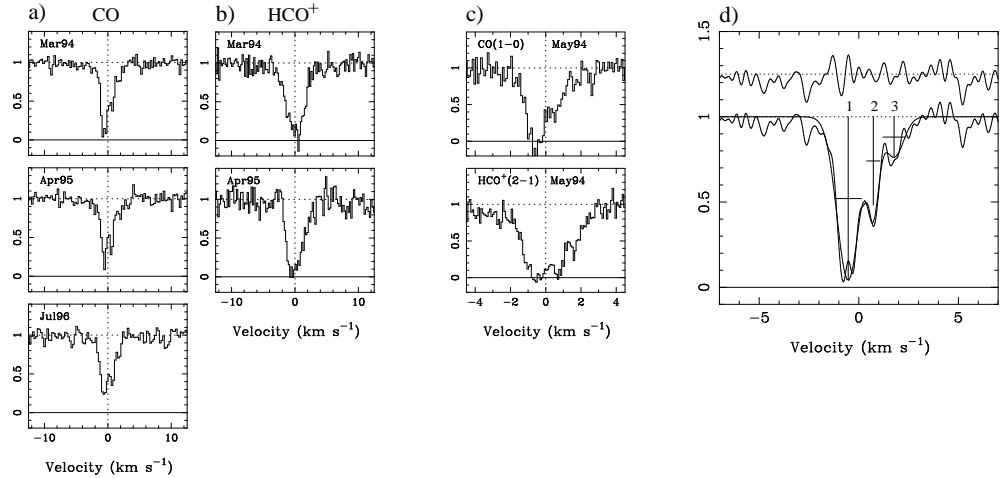


Figure 2. Absorption lines towards PKS1413+135 at different epochs. **a)** CO(1–0), **b)** HCO<sup>+</sup>(2–1). In **c)** the different line profiles of CO and HCO<sup>+</sup> are compared. **d)** Decomposition of the CO(1–0) profile into 3 gauss components.

rameters less than 0.1" (e.g. Perlman et al. 1996; Xu et al. 1995). The continuum source must therefore be situated within or near the obscuring galaxy. The small impact parameters make the latter situation highly unlikely.

*Absorption in gravitational lenses.* The two absorption line systems with the highest column densities occur in galaxies which are truly intervening and each acts as a gravitational lens to the background source: B0218+357 and PKS1830–211. In these two systems we have detected several isotopic species, showing that the main lines (at least) are saturated. Nevertheless, the absorption lines do not reach the zero level, indicating that only part of the continuum source is covered by obscuring molecular gas, but that this gas is optically thick (e.g. Combes & Wiklind 1995, Wiklind & Combes 1996a, 1997c). The lensed images of B0218+357 and PKS1830–211 consist of two main components. By comparing the depths of the saturated lines with fluxes of the individual lensed components, as derived from long radio wavelength interferometer observations, we identified the obscuration to only one of two main lensed components (Wiklind & Combes 1995; 1996a). This has subsequently been verified through mm–wave interferometer data (Menten & Reid 1996; Wiklind & Combes 1997c; Frye et al. 1997).

### 3. Small scale structure

The angular resolution of the molecular absorption line observations is set by the small, but finite, extent of the background continuum source. The size of this region decreases with increasing frequency and is located closer to the central engine than emission at lower frequencies. VLBI observations at mm–wavelengths of the flat–spectrum radio source 3C446 indicates a size  $< 30 \mu\text{arcseconds}$  (Lerner

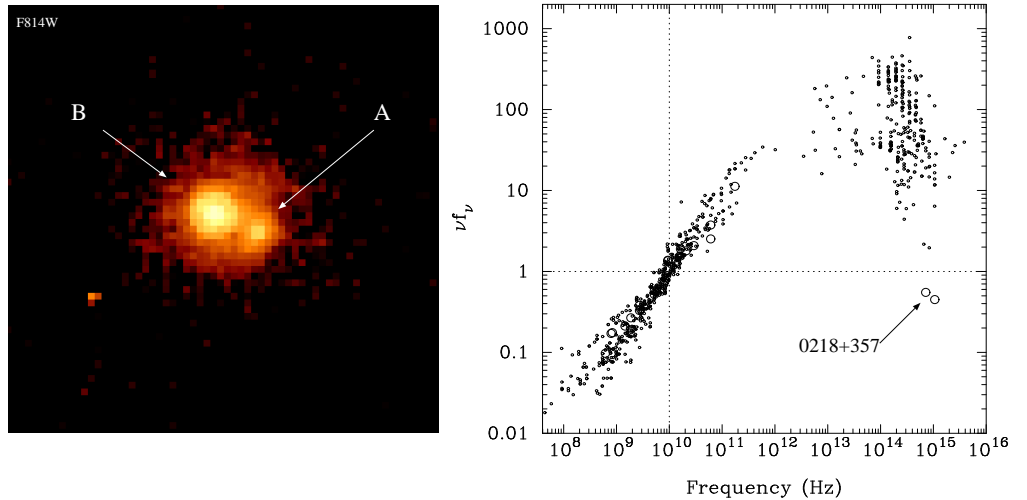


Figure 3. **Left.** HST F814W image of B0218+357. North is up, east to left. **Right.** Normalized SED for flat-spectrum radio QSOs. B0218+357 is marked by large circles.

et al. 1993), corresponding to less than 0.15 pc. The width of the absorption lines varies from less than  $1 \text{ km s}^{-1}$  (PKS1413+135) to  $\sim 30 \text{ km s}^{-1}$  (PKS1830–211). The absorption profiles are likely to consist of a superposition of several components (cf. Fig. 1a). The widths implies that each sight line samples molecular gas on parsec scales. The observed absorption line is therefore an average over  $\sim 0.1 \text{ pc}$  in extent and  $\sim 1 \text{ pc}$  in depth. If the molecular gas is structured (density and/or temperature) on these scales, it can lead to observable changes in the absorption profiles on relatively short time scales.

*PKS1413+134:* Variations have been seen in the CO(1–0) absorption line towards PKS1413+135 on a time scale of a few months (Wiklind & Combes 1997b). In Fig. 2 we show the CO(1–0) and HCO<sup>+</sup>(2–1) profiles from several epochs. Whereas the HCO<sup>+</sup> profiles remain constant to within the noise, the CO profiles exhibit changes in the depth with time. A close look reveals that it is only one of three components in the absorption profile that shows significant changes. By fitting three Gauss components to the profiles (see Fig. 2d), we found that the *ratio* of the integrated opacities of component 1 and 2 has changed by a factor  $2.3 \pm 0.3$  between May 1994 and July 1996, in the sense that component 1 had a higher opacity relative to component 2 in May 1994. The continuum flux of PKS1413+135 decreased by a factor of 3 between May 1994 and July 1996. This apparent correlation between variations and the continuum flux suggests that the variations in opacity are likely to be associated with structural changes in the AGN during an outburst. The scale of such a structural change is unknown, but likely to be very small.

There are additional features in PKS1413+135 which suggest the presence of small scale density structures in the molecular ISM. The total column density observed towards PKS1413+135 is  $N_{\text{H}} = 2N_{\text{H}_2} + N_{\text{HI}} \approx 2 \times 10^{21} \text{ cm}^{-2}$ ,

corresponding to an extinction  $A'_V \approx 2.0 \text{ mag}^1$ . This is 25 times lower than the column inferred from the deficiency of low energy X-ray photons, which implies  $A_V > 30 \text{ mag}$  (Stoche et al. 1992). Could this discrepancy be caused by an underestimate of the column density derived from the absorption lines?

When deriving the column density it is necessary to estimate the rotation temperature, i.e. the temperature governing the level population of a molecule. If it is possible to observe two transitions of the same molecule, which is usually the case, the ratio of the integrated opacities allows a derivation of the excitation temperature for these two levels. With the assumption of LTE conditions this temperature is equal to the rotation temperature. If an additional transition of the same molecule can be observed, the set of two opacity ratios should give the same excitation temperature. Towards PKS1413+135 we have observed the J=1-0, 2-1 and 3-2 transitions of HCO<sup>+</sup>. Whereas the J=2-1/1-0 ratio gives  $T_x = 5.4 \pm 0.7 \text{ K}$ , the J=2-1/3-2 ratio gives  $T_x = 8.7 \pm 0.2 \text{ K}$ . Although this discrepancy suggests that the assumption of LTE conditions does not hold, it is also compatible with LTE conditions and a multi-component gas along the line of sight, where the different components are characterized by different excitation temperatures (Wiklind & Combes 1997c). For instance, expressing the observed opacity as the sum of two components, characterized by two excitation temperatures  $T_1 < T_2$ :

$$\int \tau_\nu dV \propto N_{\text{tot}} \left( \frac{\gamma}{f(T_1)} + \frac{1-\gamma}{f(T_2)} \right) ,$$

where  $N_{\text{tot}}$  is the total column density along the line of sight,  $f$  is a function of the excitation temperature (e.g. Wiklind & Combes 1997b) and  $\gamma$  is the fraction of ‘cold’ gas (i.e.  $T_1$ ), a solution for the discrepant  $T_x$  of HCO<sup>+</sup> in PKS1413+135 is compatible with two gas components characterized by  $T_1 = 4 \text{ K}$  and  $T_2 = 18 \text{ K}$ , where  $\sim 20\%$  of the total column density originates in the cold component and the remaining  $\sim 80\%$  in the warm component. The total column density can be  $\sim 10$  times higher than the one estimated assuming a one component gas, making it more compatible with the column estimated from the deficiency of soft X-ray photons. Since the excitation of molecular gas is dominated by collisions between the molecule in question and H<sub>2</sub>, a low excitation temperature corresponds to diffuse gas, while a high excitation temperature corresponds to dense gas. This means that a two component gas as described above corresponds to a gas consisting of a dense and a diffuse part, implying structures with a large density contrast on the scales probed by the line of sight, i.e. of the order  $\sim 10^{-2} \text{ pc}^3$ .

*B0218+357* The molecular gas seen towards B0218+357 covers only one of the two lensed images of the background source (Wiklind & Combes 1995; Menten & Reid 1996). Saturated lines of both <sup>13</sup>CO and C<sup>18</sup>O have been detected, while the C<sup>17</sup>O transition remains undetected (Combes & Wiklind 1995). This gives a lower limit to the CO column density which transforms to  $N_{\text{H}_2} \approx 4 \times 10^{23} \text{ cm}^{-2}$  and an  $A'_V \approx 850 \text{ mag}$ . The absorption occurs in front of the A-component,

---

<sup>1</sup>Corrected for the redshift to correspond to  $\sim A_{3000\text{\AA}}$  using a Galactic extinction law.

which is then expected to be completely invisible at optical wavelengths. Nevertheless, analysis of archival HST data obtained with the WFPC2 in broad V- and I-band, show both components (Fig 2a). While the intensity ratio A/B of the two lensed images is 3.6 at radio wavelengths (c.f. Patnaik et al. 1996),  $A/B \approx 0.15$  at optical wavelengths. The V-I values show no difference in reddening for the A- and B-component. Hence, there are no indications of excess extinction in front of the A-component. The B-component is situated close to the center of the lensing galaxy and the optical flux from B-component is the sum of the lensed image and the nucleus of the lensing galaxy. Is the A-component an unobscured view of the background QSO, with the molecular absorption occurring elsewhere? To answer this question we compared the optical flux of the A-component (multiplied by a factor 1.3 to compensate for the B-component using the magnification ratio of 3.6) with that of similar flat-spectrum radio sources. Fluxes were taken from the literature, corrected for the redshift of the source and then normalized at the restframe frequency of 10 GHz. In Fig. 2b we plot the observed luminosities (normalized  $\nu f_\nu$  units). Despite a very large dispersion of optical luminosities for the flat-spectrum sources, the optical luminosity of B0218+357, as derived from the measured flux of the A-component, is clearly sub-luminous. This implies that, unless B0218+357 is a very peculiar source, a significant part of the optical emission region in component A is totally obscured, with  $A_V$  being very high, while a small part of it remains unobscured. Since the extent of the optical emission region is very small, this suggests the presence of very small scale structure with large density contrasts in the molecular ISM of the lensing galaxy.

#### 4. The complex absorption line system towards PKS1830–211

The radio loud QSO PKS1830–211 is lensed by an intervening galaxy and consists of two main images, designated the NE and SW images. The lensing galaxy was detected through absorption of molecular rotational lines, at a redshift  $z=0.88582$  (Wiklind & Combes 1996a). The absorption only occurs in front of the SW component. This was inferred from the depth of saturated lines and has been confirmed through mm-wave interferometric observations (Wiklind & Combes 1997c; Frye et al. 1997). A second absorbing system (designated as C in Table 1) has been identified as a 21cm HI absorption occurring at  $z=0.19$  (Lovell et al. 1996). This latter system is not seen in either molecular absorption nor emission (Wiklind & Combes 1997c). This HI absorption only occurs in front of the NE component.

A second molecular absorption system has been detected at  $z=0.88489$  (Wiklind & Combes 1997c). The new absorption line is separated by  $147 \text{ km s}^{-1}$  from the previously detected absorption (Fig. 1b) and occurs towards the NE component, in contrast to the main line which obscures the SW component. This is clearly seen in Fig. 1b, which shows the  $\text{HCO}^+(2-1)$  absorption observed with the IRAM Plateau de Bure interferometer. The spectrum is centered on the main line. The top panel shows the shift of the phase-center along the  $\alpha$ -coordinate as a function of velocity. At velocities where the continuum of the SW component is obscured by the main  $\text{HCO}^+$  absorption, the phase-center shifts towards the NE component (positive  $\alpha$ ), while the opposite is true for ve-

locities corresponding to the weaker absorption. Hence, the  $\text{HCO}^+$  absorption probes two sight lines through the intervening galaxy. Since the center of the lensing potential must be situated between the two lensed images, the velocity separation of the two absorption lines measures the rotational velocity of the gas. In order to interpret the observed velocity separation in terms of rotation, it is necessary to know where in the galaxy the sight lines occur. This can be done using existing lens models (cf. Wiklind & Combes 1997c), or through direct imaging of the lensing galaxy (see Frye, these proceedings). The second absorption system at  $z=0.885$  has also been seen in the line of  $\text{HCN}(1-0)$  and in 21cm HI absorption (Carilli et al. 1997b). The atomic fraction is higher in the NE component (weaker molecular absorption) than in the SW component, in line with the apparent correlation previously mentioned between the atomic and molecular fraction and total extinction (See Table 1).

## References

- Carilli, C.L., Perlman E.S., Stocke J.T. 1992, ApJ 400, L13  
 Carilli, C.L., Rupen, M.P., Yanny, B. 1993, ApJ 412, L59  
 Carilli, C.L., Menten, K.M., Reid, M.J., Rupen M.P.: 1997a, ApJ 474, L89  
 Carilli, C.L., Menten, K.M., Reid, M.J., Rupen, M.P., Claussen, M. 1997b, 13<sup>th</sup> IAP Colloquium: Structure and Evolution of the IGM from QSO Absorption Line Systems, eds. P. Petitjean, S. Charlot  
 Combes, F., Wiklind T. 1995, A&A 303, L61  
 Combes F., Wiklind T., 1996, in Cold Gas at High Redshift, eds. M.N. Bremer, P. van der Werf, H.J.A. Röttgering, C.L. Carilli, Kluwer Academic Pub., p. 215  
 Combes, F., Wiklind T. 1997, ApJ 486, L59  
 Frye B., Welch W. J., Broadhurst T. 1997, ApJ 478, L25  
 Lerner M., Båth L., Inoue M. et al. 1993, A&A 280, 117  
 Lovell, J.E.J., Reynolds, J.E., Jauncey D.L., et al. 1996, ApJ 472, L5  
 Lucas R., Liszt H.S.: 1994, A&A 282, L5  
 Lucas R., Liszt H.S.: 1996, A&A 307, 237  
 Menten K.M., Reid M.J.: 1996, ApJ 465, L99  
 Perlman E.S., Carilli C.L., Stocke J.T., Conway, J.S. 1996, AJ 111, 1839  
 Wiklind, T., Combes, F. 1994, A&A 286, L9  
 Wiklind, T., Combes, F. 1995, A&A 299, 382  
 Wiklind, T., Combes, F. 1996a, Nature, 379, 139  
 Wiklind, T., Combes, F. 1996b, A&A 315, 86  
 Wiklind, T., Combes, F. 1997a, A&A 324, 51  
 Wiklind, T., Combes, F. 1997b, A&A 328, 48  
 Wiklind, T., Combes, F. 1997c, ApJ in press (astro-ph/9709141)  
 Xu W., Readhead A.C.S., Pearson T.J., Polatidis A.G., Wilkinson P.N. 1995, ApJS 99, 297